ISSN 0208-7774 TRIBOLOGIA 2/2022 p. 45–53
DOI: 10.5604/01.3001.0015.9722

Krystyna RADOŃ-KOBUS*, Monika MADEJ**

PROPERTIES OF Al_2O_3 CERAMIC COATINGS APPLIED BY ALD METHOD ON 100Cr6 STEEL

WŁAŚCIWOŚCI POWŁOK CERAMICZNYCH Al_2O_3 OSADZANYCH METODĄ ALD NA STALI 100Cr6

Key words: Al_2O_3, ceramic coatings, ALD method, tribology.

Abstract: The purpose of the paper was to assess the morphology, chemical composition, geometric surface structure and contact angle, as well as to analyse the tribological properties of Al_2O_3 coatings deposited on 100Cr6 steel using the technique of atomic layers ALD. Al_2O_3 coatings were selected due to their tribological properties, adhesion to the substrate and hardness. Tribological tests were performed in a reciprocating motion in a ball-on-disc combination, with a counter-specimen of 100Cr6 steel, under the conditions of technically dry friction. Surface morphology was observed under a scanning microscope, and an EDS analyser enabled the performance of an analysis of the chemical composition of the samples. Wetting of the surface of the Al_2O_3 coating was determined by means of an optical strain gauge. The geometric surface structure before and after the tribological tests was analysed by means of a confocal microscope with an interferometric mode. The tests proved that during technically dry friction, the average coefficient of friction for the Al_2O_3 coating is lower by approximately 30% than for 100Cr6 steel. The tested coatings are characterised by hydrophobicity. Słowa kluczowe: Al_2O_3 powłoki ceramiczne, ALD, tribologia.

Słowa kluczowe: powłoki ceramiczne Al_2O_3, metoda ALD, tribologia.

Streszczenie: Celem pracy była ocena morfologii, składu chemicznego, struktury geometrycznej powierzchni, kąta zwilżania oraz analiza właściwości tribologicznych powłok Al_2O_3 osadzanych na stali 100Cr6 techniką warstw atomowych ALD. Powłoki Al_2O_3 wytypowano ze względu na ich właściwości tribologiczne, adhezję do podłoża oraz twardość. Testy tribologiczne przeprowadzono w ruchu posuwisto-zwrotnym w skojarzeniu kula–tarcza z przeciwpróbką ze stali 100Cr6 w warunkach tarcia technicznie suchego. Na mikroskopie skaningowym obserwowano morfologię powierzchni, a analizator EDS umożliwił przeprowadzenie analizy składu chemicznego próbek. Przy pomocy tensjometru optycznego określono zwilżalność powierzchni powłoki Al_2O_3. Strukturę geometryczną powierzchni przed i po testach tribologicznych analizowano za pomocą mikroskopu konfokalnego z trybem interferometrycznym. Testy wykazały, że podczas tarcia technicznie suchego średni współczynnik tarcia dla powłoki Al_2O_3 jest około 30% mniejszy niż dla stali 100Cr6. Badane powłoki charakteryzują się hydrofobowością.

INTRODUCTION

In recent years, science and technology have observed increased interest in thin coatings. This results from the ability to improve the properties of a material without changing its geometry. Among other things, these layers improve the tribocorrosion resistance of the material, its hardness or adhesion **[L. 1]**. This type of surface engineering method includes, e.g., physical vapour deposition (PVD) or chemical vapour deposition (PACVD, CVD or ALD) **[L. 2, 3]**. The atomic layer deposition (ALD)

* ORCID:0000-0003-3959-9113. Kielce University of Technology, Faculty of Mechatronics and Mechanical Engineering, Tysiąclecia Państwa Polskiego Ave. 7, 25-314 Kielce, Poland.
** ORCID:0000-0001-9892-9181. Kielce University of Technology, Faculty of Mechatronics and Mechanical Engineering, Tysiąclecia Państwa Polskiego Ave. 7, 25-314 Kielce, Poland.

method is one of the chemical deposition methods of thin layers from vapour. It is characterised by self-restriction of the layers' growth rate and the process's sequentiality. The ALD process consists of cycles, including sequentially introducing precursors into the reaction chamber. The precursors are placed therein alternately and can have a gaseous, liquid or solid form. The main advantages of the ALD method include repeatability of the process, the possibility of deposition in low temperatures, scalability of the process, no change in the geometry of the sample and precise deposition of uniform layers with a thickness measured in nanometres. The deposition of layers using the ALD method is possible even at room temperature, provided very reactive precursors are used **[L. 4]**. The main limitation for deposition using the ALD technique is the adjustment of proper reagents characterised by chemical stability in a given temperature of growth, considerable adsorption to the substrate or reaction with the substrate, and adequately high saturated vapour pressure in a given temperature of deposition. Due to the ALD method, it is possible to obtain numerous types of materials. This method is usually used to generate the following coatings: oxide (TiO_2, Al_2O_3, HfO_2 or ZnO), multi-component (ZnO:Ga, ZnO:Al.), purely metallic (Cu, Ag, Au, Pt), sulphide (ZnS) and others.

Al_2O_3 coatings are used in order to improve resistance to tribological wear **[L. 5]** and resistance to corrosion **[L. 6]**. They are also used in various combinations, e.g., with TiO_2 or ZnO coatings. Combining an Al_2O_3 coating with a TiO_2 coating provides good protection against corrosion, and their crystallisation begins at a temperature of 300°C **[L. 7, 8]**. An Al_2O_3 coating combined with a ZnO coating also contributes to the improvement of corrosion properties compared to an Al_2O_3 layer **[L. 9]**. Moreover, these coatings are characterised by biocompatibility and improved photoluminescence at room temperature **[L. 10]**. High mechanical strength is characterised by coatings generated in high temperatures **[L. 11]**. Al_2O_3 coatings are used on perovskite solar cells in order to improve their long-term stability **[L. 12]**. The present paper's purpose was to assess the tribological properties of an Al_2O_3 coating applied using the ALD method onto 100Cr6 steel.

MATERIALS AND METHOD

The research material included samples – discs 42 mm in diameter and 6 mm in height, made of 100Cr6 steel covered with an Al_2O_3 coating and 100Cr6 steel not covered with the coating. **Table 1** presents the chemical composition of 100Cr6 steel.

The coating was applied using the Atomic Layer Deposition method at a temperature of 200°C, using two precursors: water and TMA (trimethylaluminium); 2 000 cycles were used. The thickness of the coating was measured using a reflectometer, and the generated layer was approximately 200 nm thick.

Surface morphology was observed under a Phenom XL scanning microscope before and after the tribological tests, and an EDS analyser enabled the performance of an analysis of the chemical composition of the samples. The observations were performed using three magnifications: x1000, x3000, and x5000.

Table 1. Chemical composition of 100Cr6 steel [L. 13, 14]
Tabela 1. Skład chemiczny stali 100Cr6 **[L. 13, 14]**

Symbol	Fe	C	Mn	Si	P	S	Cr	Ni	Cu
wt. %	95.8– 6.7	0.95–1.1	0.25–0.45	0.15–0.35	max. 0.025	0.025	1.3– 1.65	max. 0.3	max. 0.3

The geometric surface structure before and after the tribological tests was analysed by means of a Leica DCM 8 confocal microscope with an interferometric mode, using a lens with a magnification of 20 times in the confocal mode.

The hardness of the Al_2O_3 coating was determined using the instrumental indentation method. The research used an ultra nanohardness tester from the Anton Paar Company and a Berkovich geometry indenter. A constant loading force increase rate of 2 mN/min was adopted, and a maximum load of 0.12 mN was applied.

The adhesion of the coating to the substrate was tested using the scratch test. During the test, the changes in the coefficient friction and penetration depth of the indenter were recorded in real time. The research used a nano scratch tester from the

Anton Paar Company. A linearly increasing load in a range of 0.3 to 15 mN was used, along with a scratch length of 3 mm.

The wetting of 100Cr6 steel and the Al_2O_3. coating were determined by an Attension Theta Flex optical strain gauge. The contact angle measurement involved the precise placement of a drop of the measurement liquid (distilled water and diiodomethene) with a volume of 5 µl on the sample's surface and an immediate measurement. The drops were applied to various parts of the sample, and the measurement was repeated five times.

The tribological tests were performed on an NTR^3 nanotribometer in a reciprocating motion. Spheres made of 100Cr6 steel with a diameter of 2 mm were the material constituting a counter-specimen in the tested friction pairs. Resistance to the motion was recorded during technically dry friction. The friction tests were repeated three times for each sample. The parameters of the tribological test are presented in **Table 2**.

Table 2. Parameters of the tribological test
Tabela 2. Parametry testu tribologicznego

Load [mN]	Speed [m/s]	Amplitude [mm]	Frequency [Hz]	Number of cycles	Temperature [°C]
2	0.2	5	1	10 000	25 ±2

RESULTS AND DISCUSSION

Figures 1 and **2** present surface morphologies and the spectra of characteristic X-ray radiation for 100Cr steel and the Al_2O_3 coating, respectively.

An analysis of the chemical composition of the Al_2O_3 coating confirms the chemical composition assumed in the coating generation process.

Figure 3a presents an isometric view of 100Cr6 steel, and **Figure 3b** is an isometric view of the Al_2O_3 coating generated by means of the confocal microscope with an interferometric mode. **Table 3** presents the most important amplitude parameters of the surface. The isometric view of the Al_2O_3 coating clearly indicates an improvement in the quality of the surface and a decrease in its roughness compared to 100Cr6 steel. As a result of the deposition of the Al_2O_3 coating, all amplitude surface parameters dropped by approximately 18% relative to 100Cr6 steel.

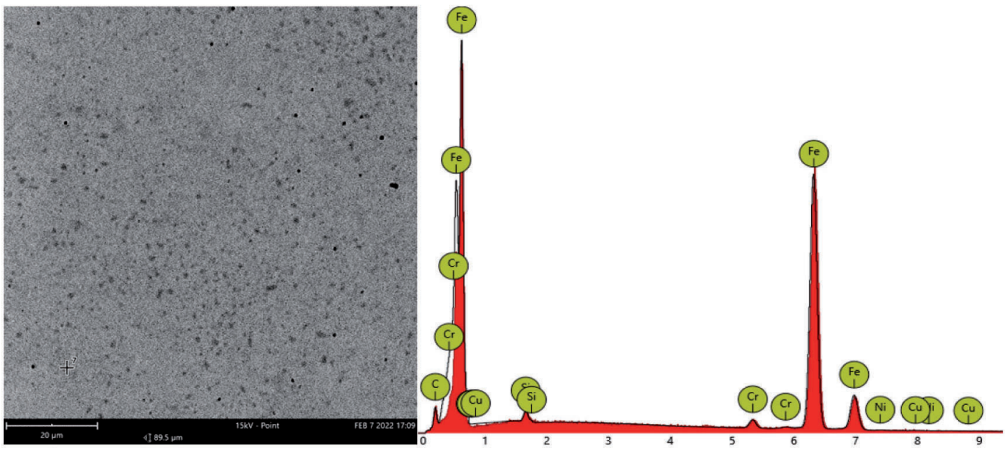

Fig. 1. Surface morphology and the spectrum of the characteristic X-ray radiation of 100Cr6 steel
Rys. 1. Morfologia powierzchni i widmo charakterystycznego promieniowania rentgenowskiego

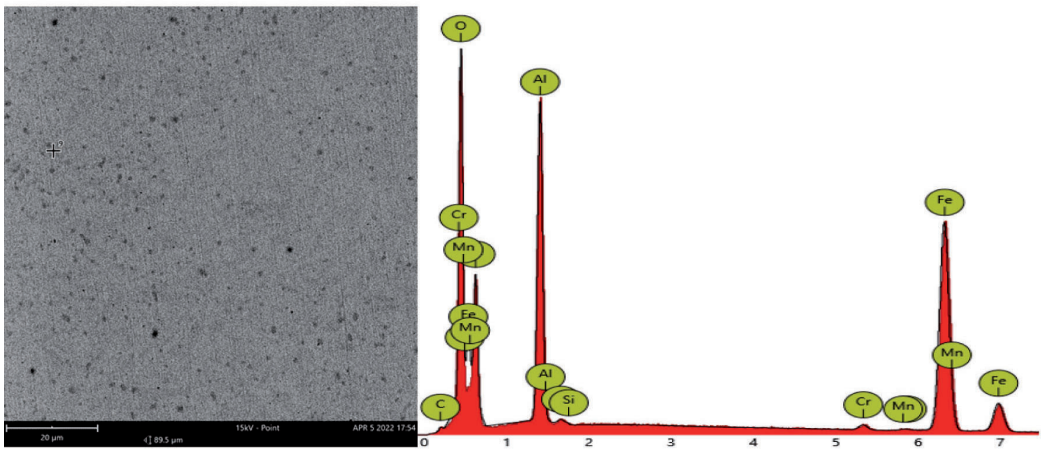

Fig. 2. Surface morphology and the spectrum of the characteristic X-ray radiation of Al_2O_3 coating
Rys. 2. Morfologia powierzchni i widmo charakterystycznego promieniowania rentgenowskiego

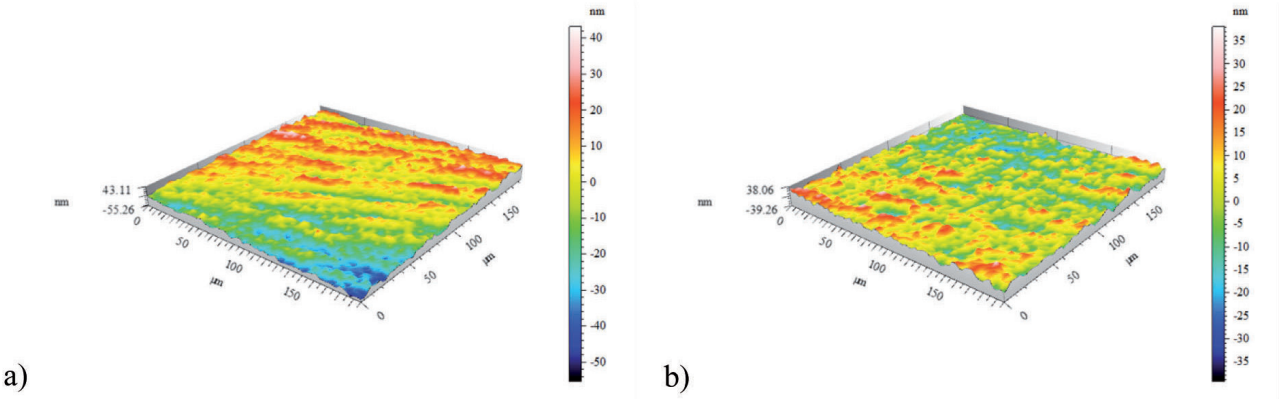

Fig. 3. Isometric view of: a) 100Cr6 steel, b) Al_2O_3 coating
Rys. 3. Widok izometryczny: a) stali 100Cr6, b) powłoki Al_2O_3

Table 3. Surface characteristic parameters
Tabela 3. Parametry amplitudowe powierzchni

Parameters	100Cr6 steel	Al_2O_3 coating
Sa [nm]	11.03	8.128
Sp [nm]	43.12	38.06
Sv [nm]	55.26	39.26
Sz [nm]	98.38	77.32
Ssk	-0.4161	0.05848
Sku	3.021	2.874

Figure 4 presents a loading and unloading curve as a function of the penetration depth of the indenter during a hardness test for the Al_2O_3 coating, as well as the mechanical parameters resulting from the performed test. Based on the produced test results, it was concluded that the Al_2O_3 coating is characterised by high resilience, evidenced by the prevalence of elastic work over plastic work. During the nanohardness test, the indenter sank to a depth of 17.5 nm, which is less than 10% of the thickness of the coating.

The measure of the adhesion of the coating to the substrate is the critical force, first causing the coating to fracture L_{Fn1}, then to spall – L_{Fn2},

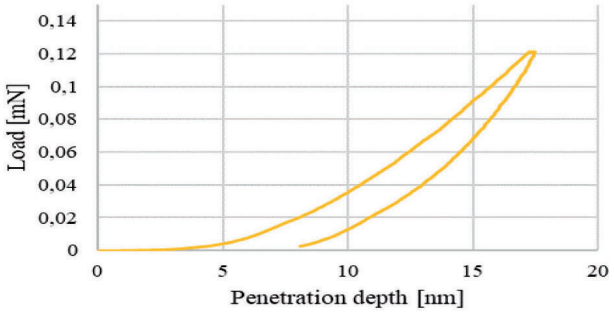

Parameters	Unit	Mean	SD
H_{IT}	GPa	9.2	0.29
E_{IT}	GPa	213.2	24.5
h_m	nm	17.5	0.45
W_{plast}	[%]	36.2	0.4
W_{elast}	[%]	63.8	0.5

Fig. 4. Loading – penetration depth curve from nanohardness tests for Al_2O_3 coating and mechanical parameters
Rys. 4. Krzywa obciążenia – głębokość penetracji wgłębnika zarejestrowana podczas testu twardości dla powłoki Al_2O_3 oraz parametry mechaniczne

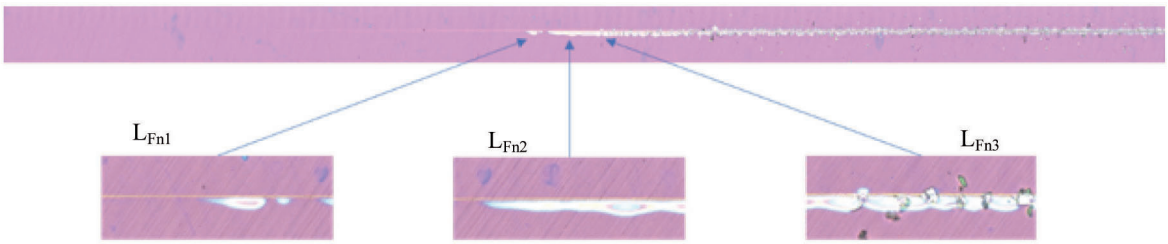

Fig. 5. View of the scratch after the scratch test for the Al_2O_3 coating
Rys. 5. Widok rysy po scratch teście dla powłoki Al_2O_3

and, as a consequence, resulting in its destruction (delamination) – L_{Fn3}. **Figure 5** presents an optical microscope image of a scratch after the scratch test for the Al_2O_3 coating **[L. 15, 16]**. **Figure 6** presents a graph of the normal force and friction coefficient as a distance function. **Figure 7** presents a graph of the penetration depth of the indenter.

The critical force was assessed based on the recorded changes in the coefficient of friction, friction force, and penetration depth of the indenter. The graphs show the characteristic points indicating the breakage of the deposited layer, and these points are marked as L_{Fn1} – L_{Fn3}. The first fractures of the Al_2O_3 coating were observed in point L_{Fn1} –

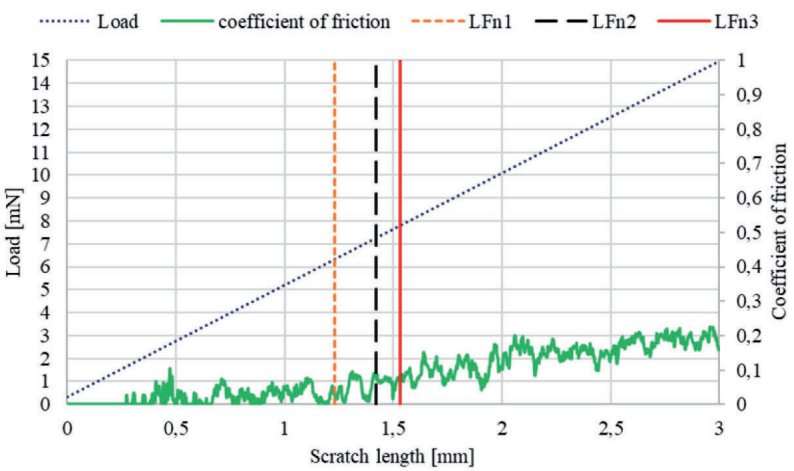

Fig. 6. Scratch test results – graph of variation of loading force (Fn), coefficient of friction (μ)
Rys. 6. Scratch test – wykres zmiany siły nacisku Fn i współczynnika tarcia

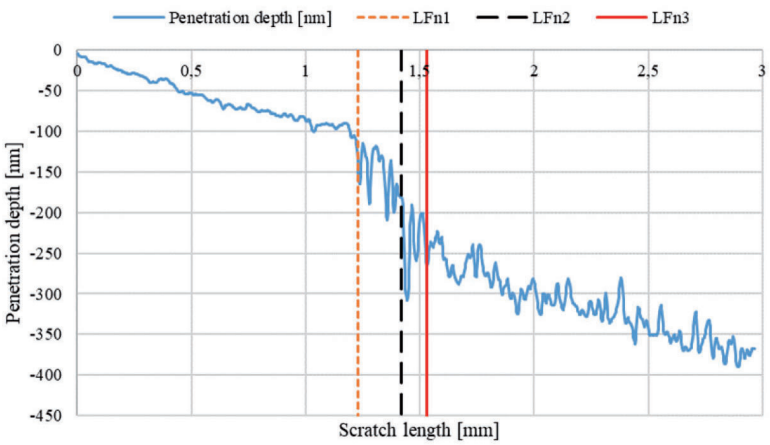

Fig. 7. Scratch test results – penetration depth of the indenter (Pd)
Rys. 7. Scratch test – głębokość penetracji wgłębnika (Pd)

6.2 mN, and larger spalling appeared in point L_{Fn2} – 7.2 mN. On the other hand, the deposited layer underwent complete breakage under a load of 7.8 mN. At this point, the sinking depth of the indenter was approximately 250 nm. Moreover, at the time of reaching the critical force of 7.8 mN, a twofold increase in the value of the coefficient of friction was observed, and this level was maintained until the end of the test.

Measurements on an optical strain gauge included recording the shape of the drop and the value of the contact angle for a drop of distilled water and diiodomethane, for 100Cr6 steel and the Al_2O_3 coating. **Figures 8** and **9** present views of the drops of measurement liquids on the surfaces of 100Cr6 steel and the Al_2O_3 coating, respectively, while **Figure 10** presents the average values of contact angles obtained in 5 measurements.

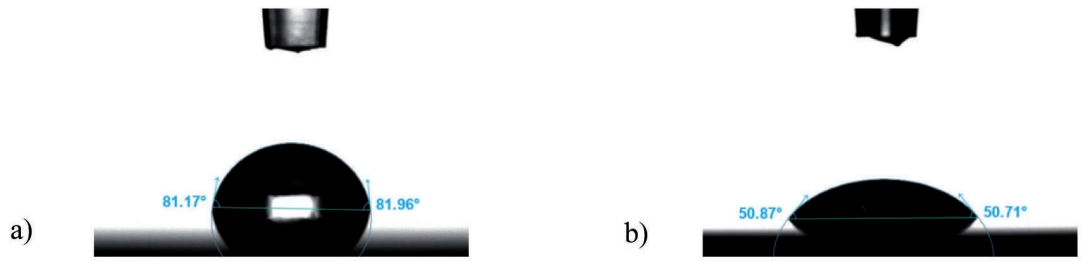

Fig. 8. A view of a drop on the surface 100Cr6 steel of: a) distilled water, b) diiodomethane
Rys. 8. Widok kropli na powierzchni stali 100Cr6: a) wody destylowanej, b) dijodometanu

Fig. 9. A view of a drop on the surface Al_2O_3 coating: a) distilled water, b) diiodomethane
Rys. 9. Widok kropli na powierzchni powłoki Al_2O_3: a) wody destylowanej, b) dijodometanu

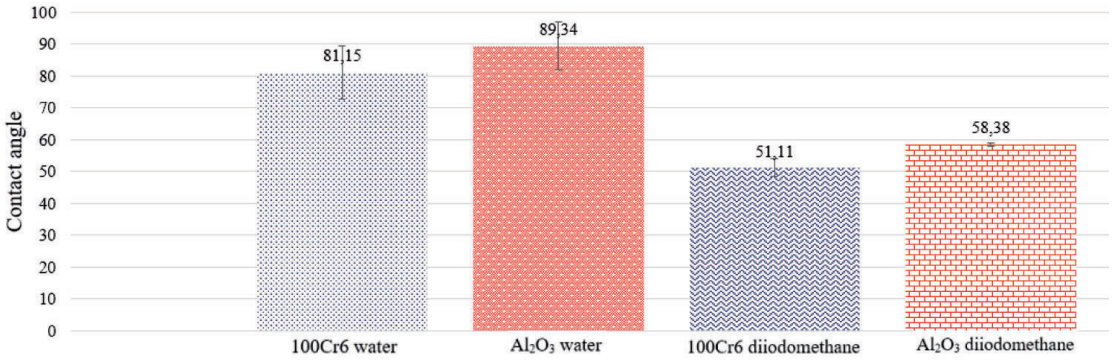

Fig. 10. The average wetting angles for 100Cr6 steel and Al_2O_3 coating
Rys. 10. Wartości średnie kątów zwilżania dla stali 100Cr6 i dla powłoki Al_2O_3

The shape of the drop of distilled water indicates that the Al_2O_3 coating is characterised by higher hydrophobicity compared to 100Cr6 steel. The contact angle measured for the Al_2O_3 coating with the use of distilled water is higher by 10% than the contact angle of 100Cr6 steel. The contact angle tested with the use of diiodomethane is also higher for the tested coating. The value of the contact angle between the Al_2O_3 coating and diiodomethane was higher by approximately 14%.

During the next research stage, tribological tests were performed under the conditions of technically dry friction. Sample trends of the recorded coefficients of friction are presented in **Figure 11** for 100Cr6 steel and the Al_2O_3 coating. The average values of the coefficients of friction for 100Cr6 steel and the Al_2O_3 coating were 0.35 and 0.24, respectively. During technically dry friction, the recorded value of the coefficient of friction for the Al_2O_3 coating was lower by approximately 30% than for 100Cr6 steel not covered with the coating.

The surface wear traces of the Al_2O_3 coating and the substrate material after tribological tests were depicted by means of the confocal microscope with an interferometric mode. **Figures 12** and **13** present the isometric images and surface profiles, taking into account wear traces for the Al_2O_3 coating and 100Cr6 steel, respectively. **Table 4** presents the values of wear indicators, i.e., the maximum depth and the abrasion area.

A higher value of the maximum depth of abrasion was recorded for 100Cr6 steel – 18 nm, while the abrasion area for 100Cr6 steel was 164 221 nm^2. For the Al_2O_3 coating, these indicators amounted to the depth of abrasion – 11 nm, abrasion area 40 267 nm^2. The width of the wear trace was also determined, amounting to 35 µm for 100Cr6 steel and 25 µm for the Al_2O_3 coating. Tests of the Al_2O_3 coating indicate that under the conditions of technically dry friction, the Al_2O_3 coating is characterised by better resistance to friction wear than 100Cr6 steel. As a result of the

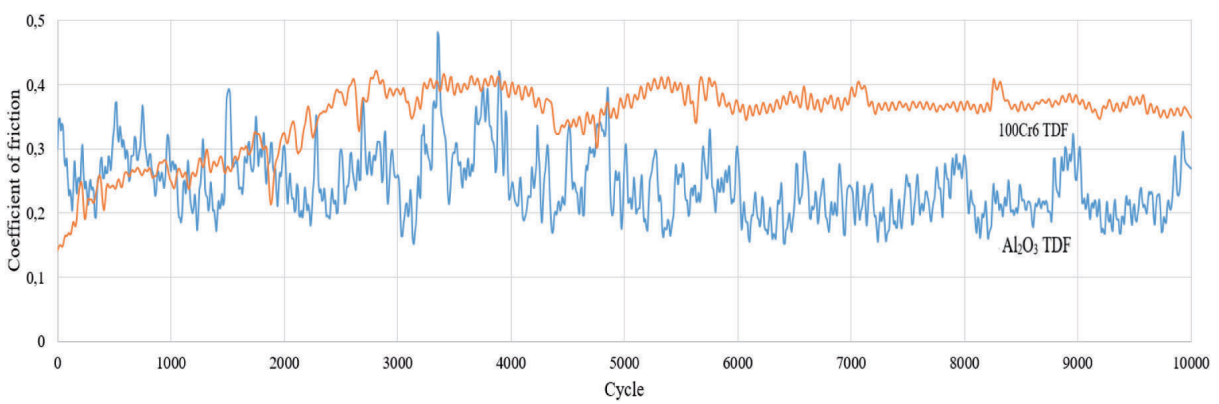

Fig. 11. Trends of sample coefficients of friction for 100Cr6 steel and the Al_2O_3 coating during technically dry friction, and the values of average coefficients of friction
Rys. 11. Przebieg przykładowych współczynników tarcia stali 100Cr6 oraz powłoki Al_2O_3 podczas tarcia technicznie suchego oraz wartości średnich współczynników tarcia

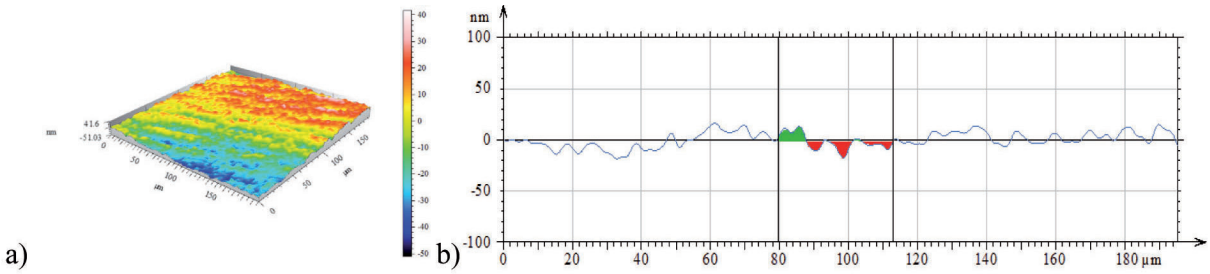

Fig. 12. The surface profiles and isometric view of the 100Cr6 steel after the technically dry friction test
Rys. 12. Profil powierzchni materiału podłoża – stali 100Cr6 oraz widok izometryczny śladu wytarcia na materiale podłoża po tarciu technicznie suchym

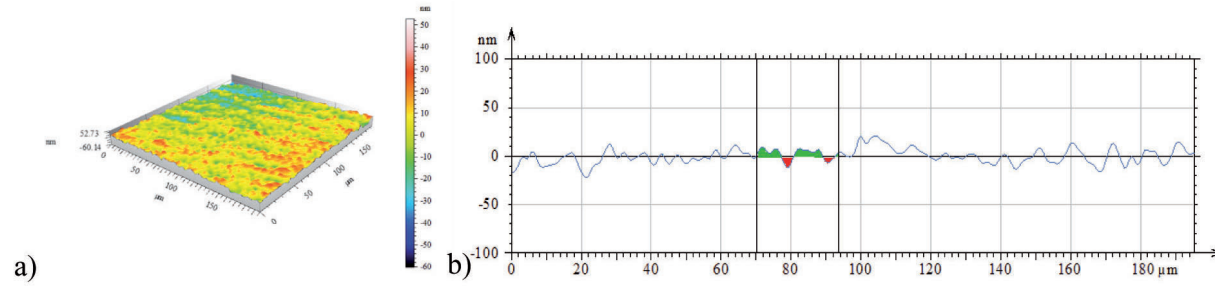

Fig. 13. The surface profiles and isometric view of the Al_2O_3 coating after the technically dry friction test
Rys. 13. Profil powierzchni powłoki Al_2O_3 oraz widok izometryczny śladu wytarcia na powłoce Al_2O_3 po tarciu technicznie suchym

Table 4. Parameters of the wear mark on the surface of Al_2O_3 coating and 100Cr6 steel after technically dry friction
Tabela 4. Parametry śladu wytarcia na powierzchni powłoki Al_2O_3 oraz stali 100Cr6 po tarciu technicznie suchym

Parameters	Unit	Steel 100Cr6	Coating Al_2O_3
Maximum depth	nm	18	11
Wear field	nm^2	164 221	40 267

used Al_2O_3 coating, the depth of abrasion decreased by 40%, and the abrasion area decreased four times compared to 100Cr6 steel.

CONCLUSIONS

The research aimed to assess the impact of Al_2O_3 coatings deposited on 100Cr6 steel using the ALD technique on the properties of unlubricated tribological systems. An analysis of the elementary chemical composition confirmed the chemical composition assumed in the process of depositing the Al_2O_3 coatings, and observations under a scanning electron microscope indicated homogeneity of the observed surfaces. During friction, a significant role is played by the geometric surface structure of the friction pair and its hardness. The resulting values of the contact angles indicate greater hydrophobicity of the Al_2O_3 coating compared to 100Cr6 steel. An analysis of the images produced on the confocal microscope and hardness measurements have indicated that 100Cr6 steel was less resistant to tribological wear than the Al_2O_3 coating. This was reflected by the results of the performed friction tests. The Al_2O_3 coating influenced a decrease in friction coefficient and wear (determined based on the wear trace: width, depth and abrasion area) compared to the substrate material – 100Cr6 steel. During technically dry friction, the average friction coefficient values were lower by approx. 30% for the Al_2O_3 coating compared to 100Cr6 steel without the coating. The tribological tests performed under the conditions of technically dry friction constitute a basis for further research. In the future, tribological tests of Al_2O_3 coatings will be performed with the use of lubricants. Al_2O_3 coatings created using the ALD technique improve the properties considerably, and they can be used in low-load tribological systems or as barrier coatings.

REFERENCES

1. Stachowiak A., Kowalski M.: Tribocorrosion performance of Cr/CrN hybrid layer as a coating for machine components, Coatings 2021, 242-1-242-16.
2. Piotrowska K., Madej M.: Influence of TiO2 coating deposited with atomic layer deposition ALD technique on the properties of Ti13Nb13Zr titanium alloy. Metalurgija 2022, pp. 665–668.
3. Milewski K., Madej M., Ozimina D.: Tribological properties of diamond like carbon coatings at friction joints lubricated with ionic liquid. Tribologia 2019, 5, pp. 59–69.
4. Martin P.M.: Handbook of Deposition Technologies for Films and Coatings, Third Edition: Science, Applications and Technology, Elsevier Inc., Amsterdam, Boston, Heidelberg, London 2010.
5. Boryło P., Lukaszkowicz K., Szindler M., Kubacki J., Balin K., Basiaga M., Szewczenko J.: Structure and properties of Al2O3 thin films deposited by ALD process. Vacuum 2016, 131, pp. 319–326.
6. Xu F., Luo L., Xiong L., Liu Y.: Microstructure and corrosion behavior of ALD Al2O3 film on AZ31 magnesium alloy with different surface roughness. Journal of Magnesium and Alloys 2020, 8, pp. 480–492.
7. Marin E., Guzman L., Lanzutti A., Ensinger W., Fedrizzi L.: Multilayer Al2O3/TiO2 Atomic Layer Deposition coatings for the corrosion protection of stainless steel. Thin Solid Films 2012, 522, pp. 283–288.
8. Gonullu M.P., Ates H.: The characteristic evolution of TiO2/Al2O3 bilayer films produced by ALD: Effect of substrate type and wide range annealing temperature. Superlattices and Microstructures 2020, 142, p. 106529.
9. Osorio D., Lopez J., Tiznado H., Farias M.H., Hernandez-Landaverde M.A., Ramirez-Cardona M., Yanez-Limon J.M., Gutierrez J.O., Caicedo J.C., Zambrano G.: Structure and surface morphology effect on the cytotoxicty of [Al2O3/ZnO]n/316L SS nanolaminates growth by Atomic Layer Deposition (ALD). Crystals 2020, 10, p. 620.
10. Chaaya A.A., Viter R., Baleviciute I., Bechelany M., Ramanvicius A., Gertnere Z., Erts D., Smyntyn V., Miele P.: Tuning optical properties of Al2O3/ZnO nanolaminates synthesised by Atomic Layer Deposition. The Journal of Physical Chemistry 2014, 118, pp. 3811–3819.
11. Lee G-B, Song S.H., Lee M-W, Kim Y-J, Choi B-H, Characterisation of physical and mechanical properties of Al2O3-doped ZnO (AZO) thin films deposited on transparent polyimide supports with various ALD process parameters. Applied Surface Science 2021, 535, p. 147731.
12. Singh R., Ghosh S., Subbiah A.S., Mahuli N., Sarkar S.K., ALD Al2O3 on hybrid perovskite solar cells: Unveiling the growth mechanism and long-term stability. Solar Energy Materials and Solar Cells 2020, 205, p. 110289.
13. 100CR6, W.NR 1.3505, EN ISO 683-17 wysokowęglowa stal łożyskowa https://steeltrans.com.pl/wyroby-stalowe/lozyskowe/100cr6-wnr-13505-en-iso-683-17/ [access: 22.03.2022].
14. ISO 683-17:2014 Heat-treated steels, alloy steels and free-cutting steels – Part 17: Ball and roller bearing steels.
15. EN 1071-3 Advanced technical ceramics – Methods of test for ceramic coatings – Part 3: Determination of adhesion and other mechanical failure modes by a scratch test.
16. ISO 14577-1 Metallic materials – instrumented indentation test for hardness and material parameters – Part 1: Test method.